1-1-2006

Continuous wave Nd:YAG laser cladding of stellite 6 multi-track layers on mild and AISI 4016 steel

M Franklin
University of Wollongong, mjf620@uow.edu.au

S W. Huang
University of Wollongong, shao@uow.edu.au

M. Brandt
Swinburne University of Technology

T Chandra
University of Wollongong, tara@uow.edu.au

A. K. Tieu
University of Wollongong, ktieu@uow.edu.au

Proceedings of the 2nd Pacific International Conference on Application of Lasers and Optics 2006

<Edited by Milan Brandt and Erol Harvey>

CONTINUOUS WAVE ND:YAG LASER CLADDING OF STELLITE 6 MULTI-TRACK LAYERS ON MILD AND AISI 4016 STEEL

M. Franklin[1], S.W. Huang[1], M. Brandt[2], T. Chandra[1], A.K. Tieu[1]

[1] Faculty of Engineering, University of Wollongong, Wollongong, NSW, 2522, Australia
[2] Industrial Research Institute Swinburne, Swinburne University of Technology
Hawthorn, Vic, 3122, Australia

Abstract

The level of sliding friction between the mating top centre and centre bowl liner components of a rail freight truck centre bearing provides both positive and negative effects on rail vehicle dynamics. Currently used centre bearing surfaces include AISI 1053 steel top centres mating against unlubricated and lubricated Hadfield steel, and polyethylene centre bowl liners. The wear life of the unlubricated AISI 1053 steel top centre against Hadfield steel is short, whilst the low friction of the lubricated and polyethylene surfaces can be detrimental to vehicle dynamics.

It is proposed to use laser clad Stellite 6 as one of the bearing surfaces. Stellite 6 multi-track layers were laser cladded on mild and AISI 4016 steel substrates with a continuous wave Nd:YAG laser at 1800 W laser source power using four different processing speeds: 600, 900, 1200, and 1500 mm/min, whilst the laser power, defocused laser spot size, and powder feed rate were constant. The cladding samples were characterised using optical microscopy and scanning electron microscopy (SEM) in conjunction with energy dispersive spectroscopy (EDS). Microhardness profiles of the cladded layer and heat affected zone were determined. The effect of processing speed on cladded layer height, depth of penetration and dilution has been examined. The main difference between the samples clad onto the two different substrates was the microstructure and hardness of the heat affected zone. Untempered martensite was observed in the heat affected zone of the AISI 4016 steel substrate at 1500 mm/min. For both substrates the optimum processing speed is between 600 and 900 mm/min.

1. Introduction

Laser cladding is commonly used for hardfacing applications to melt a powder of one metal alloy or metal matrix composite onto steel thus improving the surface properties of the materials. The controlled heat input from the laser ensures a fusion bond with minimal dilution of the clad layer by elements from the steel substrate [1]. Stellite 6 has good unlubricated wear resistance [2]. For applications involving both dry sliding wear and impact loading, such as in a rail freight bogie centre bearing, it is important that the substrate has high fracture toughness. For such an application quench and tempered AISI 4016 molybdenum steel would be suitable.

In this paper, stellite 6 powder has been laser cladded on mild and quench and tempered AISI 4016 steels at four different processing speeds. The aim is to determine the effect of processing speed on the clad height, depth of penetration, level of dilution, microstructure and hardness.

2. Experimental details

2.1 Materials

The stellite 6 powder used had the particle size in the range of 45-75 μm. The substrates used were mild and quench and tempered AISI 4016 steels with thickness of 10 and 6 mm, respectively. The nominal chemical compositions of the stellite 6 powder and steel substrates are listed in Table 1.

Table 1. The nominal chemical composition of stellite 6 powder and the steel substrates.

	C	Cr	Si	W	Fe	Co	Ni	Mn	Mo
Stellite 6	1.13	29.20	1.39	4.65	2.37	58.29	2.37	0.26	0.34
Mild steel	0.20	0.20	0.23	-	98.80	-	-	0.57	-
AISI 4016 steel	0.16	0.02	0.20	-	98.19	-	0.03	1.10	0.22

2.2 Laser cladding

Laser cladding was performed with a Nd:YAG laser operated at 1800 W laser source power in continuous wave mode. The laser beam was delivered to the workpiece via a 10 m long, 0.6 mm diameter, silicon optical fiber with a numerical aperture of 0.22. From the fiber, the beam passed through a 50 mm diameter, 200 mm focal length collimating lens. Then it was reflected off a 45° bending mirror and then focused through a 50 mm diameter, 200 mm focal length focusing lens. The focal spot was positioned 20 mm above the workpiece which resulted in the defocused laser spot size on the workpiece being 4.0 mm. A pneumatic powder feeder using argon as the carrier and shielding gas delivered the alloy powder to the laser melting pool on the workpiece through a side injecting nozzle. The powder feed rate was 20.5 g/min. The workpiece was mounted on a CNC table which can move in both the X- and Y-directions at a controllable speed. Four processing speeds were used: 600, 900, 1200 and 1500 mm/min. Multi-track clads were made with 14 tracks of 27 mm length laid side by side using an increment of 1.5 mm (Figure 1).

For these experiments the laser power, laser spot size and powder feed rate are fixed. The delivered powder mass flow and laser energy per clad track length decrease as the processing speed increases as presented in Table 2. These parameters will be used to discuss the results.

Table 2. Delivered powder mass flow and laser energy per clad track length as a function of processing speed.

Processing speed (mm/min)	Delivered powder mass flow per clad track length (mg/mm)	Delivered laser energy per clad track length (J/mm)
600	34.2	180
900	22.8	120
1200	17.1	90
1500	13.7	72

2.3 Metallurgical characterisation

Surface cracks and pores were assessed using the dye-penetrant test. The clad samples were sectioned (Figure 1), mounted, polished to a 1 μm finish and then etched in 2.5% nital to reveal the microstructure of the cladded layer, heat affected zone and substrate. Microstructural observations were carried out using Leica optical and Stereoscan 440 scanning electron microscopes (SEM). The cladded layer thickness and depth of penetration were measured using optical microscopy. The elemental analysis of the cladded layer and substrate were measured using an energy dispersive spectrometer (EDS) attached to the SEM and used in the spot scan mode. These results were used to calculate the dilution level of the cladded layer.

Microhardness was measured across the cladded layer, heat affected zone and substrate using a microhardness testing machine at a load of 100 g. The cladded layer thickness, depth of penetration, EDS and hardness were measured in the region of the 8th cladding track as shown in Figure 2.

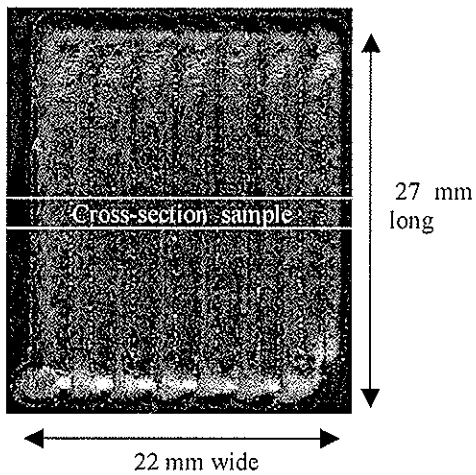

Figure 1. Multi-track clad sample showing dimensions and location of cross-section sampling.

3. Results

The surface appearance of the laser cladded stellite 6 layer on mild steel at a processing speed of 900 mm/min is shown in Figure 1. This is typical for all samples. Dye-penetrant testing showed all samples to have a crack- and porosity-free surface. The cross-section of the laser cladded layer is shown in Figure 2. It shows that the cladded layer thickness is reasonably even across the width. However, there is some inter-track porosity and the depth of penetration, apart from the first track, is only significant from the seventh track onwards.

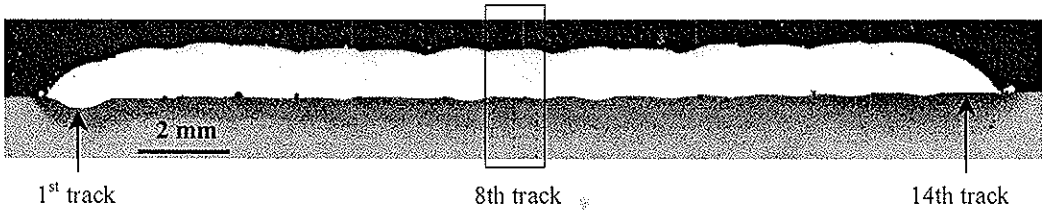

Figure 2. Cross-section of multi-track clad showing cladding tracks and heat affected zone. Energy dispersive spectroscopy and hardness measurements made within the 8th cladding track.

This appears for all the samples treated at 900, 1200 and 1500 mm/min. However, for the samples treated at 600 mm/min the samples show two differences: there is significant inter-track porosity and the cladded layer does not penetrate below the substrate surface.

The measured cladded layer thickness and depth of penetration are presented in Table 3. As the processing speed increases the cladded layer thickness decreases. The depth of penetration increases as the processing speed increases from 600 to 1200 mm/min, however then decreases at 1500 mm/min.

Table 3. Cladded layer thickness and depth of penetration at various processing speeds and for the two steel substrates.

Substrate	Processing speed (mm/min)	Clad height (mm)	Depth of penetration (μm)
Mild steel	600	1.60	0
	900	1.06	25
	1200	0.77	145
	1500	0.66	60
AISI 4016 steel	600	1.74	0
	900	1.24	-
	1200	0.90	125
	1500	0.70	15

The dilution profiles of the cladded layers at different processing speeds are shown in Figures 3 and 4 for the mild and AISI 4016 steel substrates, respectively. The general trends for both substrates are similar and will be presented collectively. The dilution at 50 μm depth for substrates clad at 900 and 1200 mm/min is between 11-16%. At depth of 150 μm to near the surface of the clad the dilution for the various processing speeds follows the same trend discussed previously for depth of penetration. At a processing speed of 600 mm/min the dilution is negligible. With increasing processing speed the dilution increases to 2-6% at 900 mm/min, then further to 7-11% at 1200 mm/min, then decreases to 1-5% at 1500 mm/min.

The microstructure comprises mostly primary dendrites of the cobalt rich phase (γ, face-centred cubic) and interdendritic eutectic. Some dendritic segregation or coring was present in all microstructures. The microstructure for up to several tens of microns next to the fusion boundary is typical of planar interface solidification [3]. Cellular dendritic structures [3] were also observed particularly near the fusion boundary. For the mild and AISI 4016 steel substrates, the dendrite size of the clad at a processing speed of 600 mm/min (Figure 5) was significantly greater than at the other speeds (Figure 6), which were all similar. The heat affected zone in the AISI 4016 substrate at a processing speed of 1500 mm/min comprised untempered and tempered martensite near the fusion boundary, whereas at other speeds it comprised solely tempered martensite.

The microhardness at various depths of the substrate, heat affected zone and cladded layer for different processing speeds are shown in Figures 3 and 4 for the mild and AISI 4016 steel substrates, respectively. The thickness of the heat affected zone for the mild steel substrates was 0.75 mm. For the AISI 4016 substrates, it was 1.55 mm for the samples cladded at 600 and 900 mm/min, and 0.95 mm for the samples cladded at 1200 and 1500 mm/min.

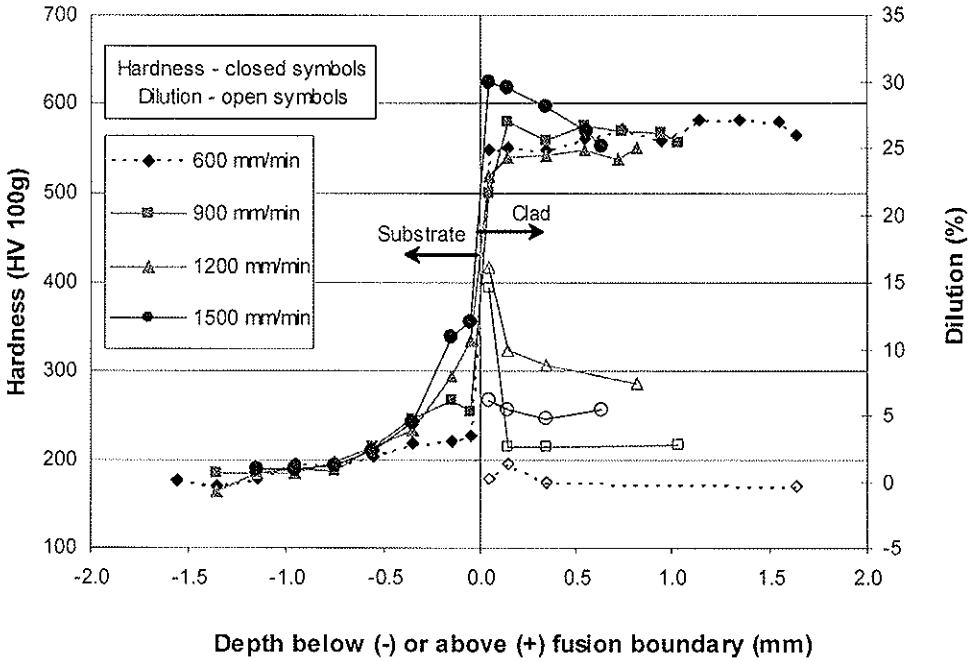

Figure 3. Dilution profiles across cladded layers and microhardness profiles across cladded layers and heat affected zones for mild steel substrate samples at different processing speeds.

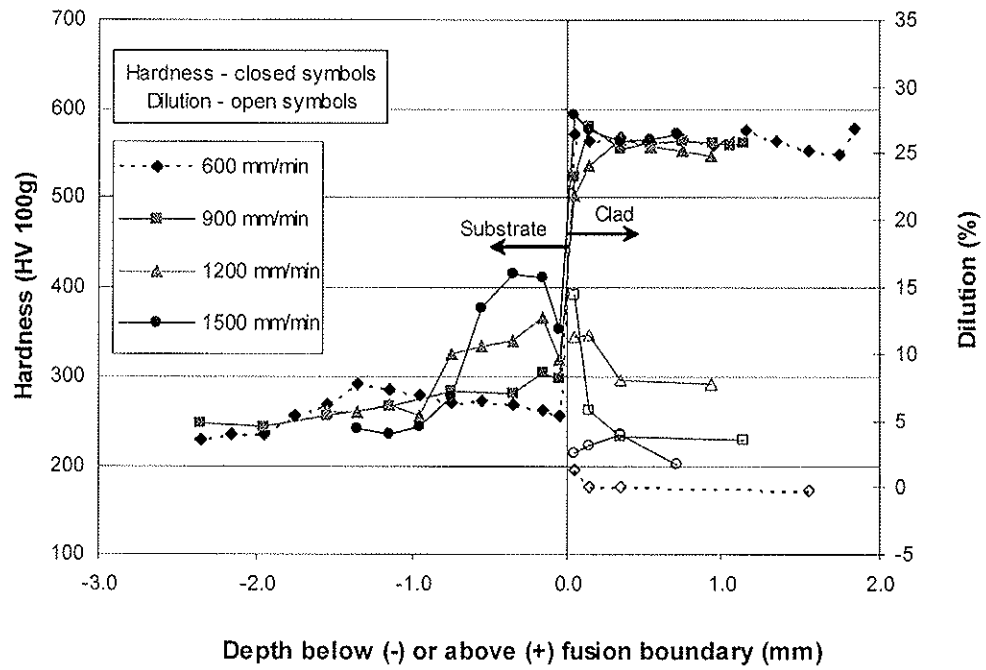

Figure 4. Dilution profiles across cladded layers and microhardness profiles across cladded layers and heat affected zones for AISI 4016 steel substrate samples at different processing speeds.

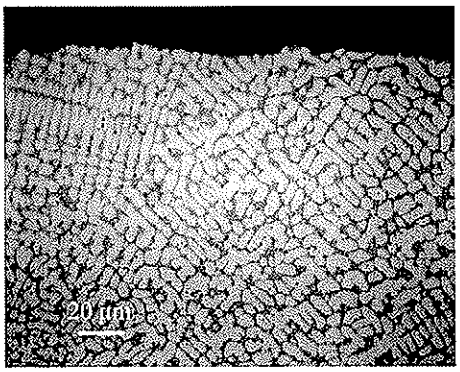

Figure 5. Microstructure of the cladded layer on AISI 4016 steel at 600 mm/min processing speed.

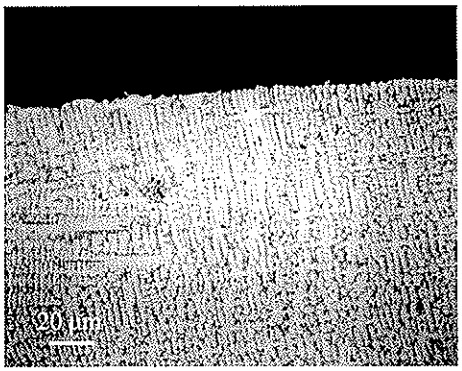

Figure 6. Microstructure of the cladded layer on AISI 4016 steel at 900 mm/min processing speed.

The maximum hardness reached in the heat affected zone of the AISI 4016 steel substrates was 415 HV for the sample cladded at 1500 mm/min processing speed.

The samples at 900 and 1200 mm/min showed some low hardness values within the cladded layer near the fusion boundary ranging from 500 and 536 HV. The cladded layers at 1500 mm/min showed very high hardness especially near the fusion boundary. Apart from these results, for the mild and AISI 4016 steel substrates, the hardness range of the cladded layer was 537-581 and 546-577 HV, respectively.

4. Discussion

The high narrow bead profile that forms at a processing speed of 600 mm/min is due to the high delivered powder mass flow per clad track length and largely causes the observed inter-track porosity [1]. At this same speed the observed lack of penetration into the substrate surface is due to laser power attenuation by the high delivered powder mass flow per clad track length [4].

The decrease in cladded layer thickness with increasing processing speed is due to the corresponding decrease in delivered powder mass flow per clad track length.

As the processing speed increases from 600 to 1200 mm/min both the depth of penetration and dilution increases, then with further increase to 1500 mm/min they decrease. The dilution is related to the measured depth of penetration and cladded layer thickness. As the depth of penetration increases for a given cladded layer thickness there is more molten iron available for diffusion into the cladded layer and subsequently higher dilution results. The observed trend for dilution against processing speed is in agreement with the thesis by Salehi who showed the same trend for nickel based (Hastelloy C) alloy powder cladded on mild steel for laser powers of 1500 and 1700 W and processing speeds ranging from 600 to 1600 mm/min [5]. However, for the same processing speed range at a higher laser power of 1900W, with increasing processing speeds up to 1600 mm/min it was found that the dilution continued to increase without decreasing. [5]. In these present experiments, at a processing speed of 600 mm/min the high delivered powder mass flow per clad track length attenuates the laser power so less energy is absorbed by the substrate. At increasing speeds to 1200 mm/min, laser power attenuation is reduced and more energy is available for substrate melting explaining the observed increase in depth of penetration, and subsequent dilution. As the processing speed is increased further to 1500 mm/min the decrease in depth of penetration, and corresponding dilution, could be explained by the further reduced delivered laser energy per clad track length and/or insulating effect of powder which is likely to be less dense than at lower processing speeds [6].

The microstructures of the clad layers are typical of those observed previously [7-9]. The coarser dendrite size for the samples clad at 600 mm/min compared to the other processing speeds is due to the longer interaction time and lower cooling rate. The rapid cooling rate associated with the cladding on AISI 4016 steel at 1500 mm/min has led to the presence of untempered martensite near the fusion boundary.

The relatively low hardness within the cladded layer near the fusion boundary for the samples at 900 and 1200 mm/min is due to high dilution

in excess of 8% [10]. The very high hardness of cladded layers at 1500 mm/min especially near the fusion boundary is primarily due to high residual stresses from high cooling rate, and secondary factors are the fine dendrite size and low dilution. Similarly, for the AISI 4016 substrate the high cooling rate has resulted in the formation of untempered martensite in the heat affected zone. The toughness of this substrate would be significantly reduced as a result.

For both substrates the optimum processing speed is between 600 and 900 mm/min. This should provide a cladded layer with low dilution and residual stresses, and an acceptable heat affected zone providing a high hardness and low dilution.

5. Conclusions

The following conclusions can be drawn about this study:

(1) The clad height decreases with increasing processing speed.

(2) The depth of penetration, and subsequently dilution, increases with increasing processing speed to 1200 mm/min, and then decreases at 1500 mm/min processing speed.

(3) The hardness of the cladded layer is reduced at dilution levels greater than 10%.

(4) Untempered martensite forms in AISI 4016 when clad at 1500 mm/min.

(5) For both substrates the optimum processing speed is between 600 and 900 mm/min.

Acknowledgements

The paper is supported by the Cooperative Research Centre for Railway Engineering and Technologies of Australia (Rail CRC) Theme 1: Smart Train System. Many thanks to Mr Scott Simson, the project leader, for his support of this work in many ways. Thanks to Mr Bruce Brymer and Mr Jonathan Grose of Queensland Rail for their ongoing support and interest in this work, and for providing the AISI 4016 steel substrates used in this research.

We would like to thank Mr Jim Harris for taking the time to produce the laser clad samples used in this work.

References

[1] Weerasinghe, V.M. & Steen, W.M. (1983) Laser cladding with pneumatic powder delivery, in Proceedings of the American Society of Metals: Lasers in Materials Processing, Metals Park, Ohio, USA, 166-174.

[2] Crook, P., & Farmer, H.N. (1992) Friction and wear of hardfacing alloys, Henry, S.D. (ed) ASM Handbook: Friction, lubrication, and wear technology, Vol 18, ASM International, 758-765.

[3] Kurz, W, & Stefanescu, D.M. (1988) Principles of solidification, in Davis, J.R. (ed) ASM Handbook: Casting, Vol 15, ASM International, 101-182.

[4] Sun, S., Durandet, Y., & Brandt, M. (2005) Parametric investigation of pulsed Nd:YAG laser cladding of stellite 6 on stainless steel, Surface & Coatings Technology 194, 225-231.

[5] Salehi, D. (2005) Sensing and control of Nd:YAG laser cladding process, Ph.D. thesis, Swinburne University of Technology, Australia.

[6] Huang, S.W. (2000) Tribological performance and microstructure of physical vapour deposition coatings, laser clad WC/Ni layers and duplex coatings, Ph.D. thesis, University of Wollongong, Australia.

[7] De Mol van Otterloo, J.L., De Hosson, J.T.M. (1996) Microstructure and abrasive wear of cobalt-based laser coatings, Scripta Materialia 36, No.2, 239-245.

[8] D'Oliveira, A.S.C.M., Da Silva, P.S.C.P., Vilar, R.M.C., (2002) Microstructural features of consecutive layers of Stellite 6 deposited by laser cladding, Surface and Coatings Technology 153, 203-209.

[9] Mingxi, L., Yizhu, H., Guoxiong, S., (2004) Microstructure and wear resistance of laser clad cobalt-based alloy multi-layer coatings, Applied Surface Science 230, 201-206.

[10] Yellup, J.M. (1995) Laser cladding using the powder blowing technique, Surface and Coatings Technology 71, 121-128.